LAGRANGIAN DISPERSION MODEL BASED ON ELLIPTIC RELAXATION IN THE ATMOSPHERIC BOUNDARY LAYER

Byunggu Kim, Changhoon Lee
Department of Mechanical Engineering,
Yonsei University
134 Shinchon-dong, Seodaemun-gu, Seoul, 120-749, Korea
kbg73@yonsei.ac.kr, clee@yonsei.ac.kr

ABSTRACT

A new simple Lagrangian dispersion model for neutral atmospheric boundary layer is proposed. A version of the Generalized Langevin equation corresponding to the Isotropization of Production Reynolds stress model is applied to horizontally homogeneous equilibrium turbulent boundary layer. Constrains for the model constants are derived from the self-similarity condition of near-wall turbulence. The proposed model is tested for the prediction of dispersion due to a point source in two dimensions and compared with available experimental data and other well-known models.

INTRODUCTION

An important issue in environmental science is prediction of air pollution in the atmospheric boundary layer. Several Lagrangian dispersion models in neutral turbulent boundary layer have been proposed by many authors and are well documented in Kurbanmuradov & Sabelfeld(2000). The main difficulty in Lagrangian modeling comes from the inhomogeneity of turbulence near the wall where pollutant is typically released. Thomson(1986) proposed a criteria, the so-called well-mixed condition, for the Lagrangian dispersion model in turbulent flows. Thomson's model(1986), Reynolds's model(1998b) and Kurbanmuradov & Sabelfeld's model(2000) belong to the well-mixed class. The well-mixed condition, however, cannot provide a unique dispersion model in three dimensions. Dreeben and Pope(1997, 1998) proposed a Lagrangian stochastic model for the calculation of turbulent flow itself and successfully applied to turbulent channel flow at row Reynolds number. In this study we use the GLM (generalized Langevin model)(Haworth and Pope, 1986) corresponding to the Isotropization of Production Model (Pope, 1994) and the elliptic-relaxation method to develop a new dispersion model which is applicable to horizontally homogeneous boundary layer flow. The general solution of the elliptic relaxation is not trivial, but the approximate solution under the self-similarity assumption for the near-wall turbulence is easily attainable. A further application of the self similarity significantly simplifies the model by yielding constraints for the model constants, resulting in a simple dispersion model in closed form. The performance of the proposed model is examined through comparison with experimental data by Raupach and Legg (1983) and predictions of other models.

DISPERSION MODEL

Generalized Langevin Equation

The Lagrangian particle velocity U_i is decomposed into its mean and fluctuating component

$$U_i = \langle U_i \rangle + u_i \tag{1}$$

where $\langle \cdot \rangle$ denotes the Eulerian mean at particle position. For infinitesimal time increment dt, each particle's position $X_i(t)$ evolves according to

$$dX_i = U_i dt \tag{2}$$

In high Reynolds number flow, viscosity of fluid can be neglected. Hence, The generalized Langevin model of Haworth and Pope (1986) specifies velocity of modeled particles,

$$du_i = G_{ij} u_j dt + \sqrt{C_0 \epsilon}\, dW_i \tag{3}$$

where dW_i is an increment of the Wiener process with zero mean and variance dt. C_0, ϵ are Kolmogorov's constant and mean dissipation rate, respectively. It should be noted that the model equation is for the fluctuating component rather than the total Lagrangian particle velocity. The anisotropic effect is incorporated into the model by modeling of the drift term G_{ij} (Dreeben and Pope, 1998):

$$G_{ij} = \frac{g_{ij} - \frac{1}{2}\epsilon \delta_{ij}}{k} \tag{4}$$

Here, k denotes turbulent kinetic energy. In this study, the nonlocal effect near the wall is realized by the elliptic relaxation model of g_{ij}:

$$g_{ij} - L^{2-p-q} \nabla \cdot [L^p \nabla (L^q g_{ij})] = \overline{g_{ij}} \tag{5}$$

where $\overline{g_{ij}}$ is the local model specified by

$$\overline{g_{ij}} = \frac{1 - C_1}{2} \epsilon \delta_{ij} + k H_{ijkl} \frac{\partial \langle U_k \rangle}{\partial x_l} \tag{6}$$

where C_1 corresponds to the model constant from Rotta's Return-to-Isotropy model if the second term is absent and H_{ijkl} denotes a fourth-order tensor representing anisotropy of Reynolds stress,

$$H_{ijkl} = (C_2 + \frac{1}{3}\gamma_5)\delta_{ik}\delta_{jl} - \frac{1}{3}\gamma_5 \delta_{il}\delta_{jk} + \gamma_5 b_{ik}\delta_{jl} - \gamma_5 b_{il}\delta_{jk} \tag{7}$$

where C_2 and γ are the model constants for the Isotropization of Production Model(IPM) and b_{ij} is anisotropy tensor

defined by $b_{ij} = \langle u_i u_j \rangle / \langle u_k u_k \rangle - \delta_{ij}/3$ and the length scale is specified by

$$L = C_L \frac{k^{3/2}}{\epsilon} \tag{8}$$

Solution of Elliptic Relaxation

g_{ij} is a solution of an elliptic differential equation and it is generally costly to find a solution in a domain with arbitrary boundaries. In the boundary layer flow, however, the self-similarity assumption can greatly simplify the solution procedure. Furthermore, the effect of viscosity is not considered, thus eliminating the singularity at the wall. The consequence of this is that the boundary condition is not necessary and only the particular solution of Eq. (5) needs to be considered. The assumption we make is that turbulent statistics near the wall are self similar which implies

$$\langle U(y) \rangle = \frac{u_\tau}{\kappa} \ln \frac{y}{y_0} \tag{9}$$

$$\epsilon(y) = \frac{u_\tau^3}{\kappa y} \tag{10}$$

$$\langle u^2 \rangle = a^2 u_\tau^2,\ \langle v^2 \rangle = b^2 u_\tau^2,\ \langle w^2 \rangle = c^2 u_\tau^2 \tag{11}$$

$$\langle uv \rangle = -u_\tau^2 \tag{12}$$

where y and u_τ denote the distance from the wall and the wall-shear velocity, respectively. u, v and w is the streamwise, wall-normal and spanwise velocities, respectively. κ is von Karman constant and y_0 is the roughness length scale. The constants are $a = 2.5, b = 1.25, c = 2.0, \kappa = 0.41$. Then $\overline{g_{ij}} \sim 1/y$ and $L \sim y$, resulting in closed form solution for g_{ij},

$$g_{ij} = \frac{\overline{g_{ij}}}{R} \tag{13}$$

with

$$R = 1 - C_L^2 \kappa^2 \left(\frac{a^2 + b^2 + c^2}{2} \right)^3 (q-1)(p+q-2) \tag{14}$$

This means that the nonlocal modification is equivalent to a simple rearrangement of the model constants. Note that when $q = 1$ or $p + q = 2$, the nonlocal effect vanishes. We set p to 0 and q to 1. Consequently, $R = 1$ and g_{ij} has the same form as the local model.

$$g_{ij} = \overline{g_{ij}} \tag{15}$$

Constraints for Model Constants

GLM can be written for the modeled Lagrangian velocity u^*:

$$du_i^* = G_{ij} u_j^* dt + \sqrt{C_0 \epsilon} dW_i \tag{16}$$

Here, G_{ij} and ϵ are specified by the self-similarity conditions Eqs. (9) $\sim$ (12). Therefore, the modeled Reynolds stresses should satisfy this self similarity. Multiplying (16) by velocity component and using the Ito calculus yield

$$\frac{d\langle u_i u_j \rangle^*}{dt} = G_{ik} \langle u_j u_k \rangle^* + G_{jk} \langle u_i u_k \rangle^* + C_0 \epsilon \delta_{ij} \tag{17}$$

where $\langle u_i u_j \rangle^*$ denotes the modeled Reynolds stress. Note that Eq. (17) does not contain the production term. The reason for this is that the total Lagrangian velocity is not considered in the present Lagrangian model and the inhomogeneity of the mean flow is not explicitly taken into account.

Table 1: Constraint of constant

fixed quantity	Constraint
$\langle u^2 \rangle, \langle v^2 \rangle$	$C_1 = \frac{k}{b^2 u_\tau^2} C_0,\ C_2 = -(\frac{a^2}{b^2} - 1)\frac{C_0}{2}$
$\langle uv \rangle, \langle v^2 \rangle$	$C_1 = \frac{k}{b^2 u_\tau^2} C_0,\ C_2 = -\frac{1}{b^4} C_0$

For the self similarity, $\langle u^2 \rangle^* = \langle u^2 \rangle$, $\langle v^2 \rangle^* = \langle v^2 \rangle$, $\langle uv \rangle^* = \langle uv \rangle$, yielding the following constraints:

$$-\frac{1}{k} C_1 \epsilon \langle u^2 \rangle + 2 C_2 \frac{d\langle U \rangle}{dy} \langle uv \rangle + C_0 \epsilon = 0 \tag{18}$$

$$-\frac{1}{k} C_1 \epsilon \langle v^2 \rangle + C_0 \epsilon = 0 \tag{19}$$

$$-\frac{1}{k} C_1 \epsilon \langle uv \rangle + C_2 \frac{d\langle U \rangle}{dy} \langle v^2 \rangle = 0 \tag{20}$$

It should be noted that γ_5 vanishes during opertaion, suggesting that the role of γ_5 is not redistribution between the Reynolds stresses. Investigation reveals that γ_5 is strongly related to the rotational property of particle motion. Eqs. (18) $\sim$ (20) do not uniquely determine the model constants C_0, C_1 and C_2 except the trivial solution, $C_0 = C_1 = C_2 = 0$. Therefore the present model is incomplete in terms of the model constants. However, if we relax the constraint, a partially complete model can be derived. This can be achieved if we select only two quantities among three stresses which are maintained to be the same as the given values. For example, the resulting expressions between C_0, C_1 and C_2 for two choices of fixed Reynolds stresses are listed in Table 1. Satisfaction of these constraints, however, does not guarantee that the desired Reynolds stresses remain to be the same values as the given ones. Let us assume the model satisfying $\langle v^2 \rangle^* = \langle v^2 \rangle$, $\langle uv \rangle^* = \langle uv \rangle$, then

$$-\frac{1}{k} C_1 \epsilon \langle u^2 \rangle^* + 2 C_2 \frac{d\langle U \rangle}{dy} \langle uv \rangle + C_0 \epsilon - \gamma_5 \frac{\langle uv \rangle}{k} \frac{d\langle U \rangle}{dy} (\langle u^2 \rangle^* - \langle u^2 \rangle) = 0 \tag{21}$$

$$-\frac{1}{k} C_1 \epsilon \langle v^2 \rangle + C_0 \epsilon = 0 \tag{22}$$

$$-\frac{1}{k} C_1 \epsilon \langle uv \rangle + C_2 \frac{d\langle U \rangle}{dy} \langle v^2 \rangle - \frac{\gamma_5}{2k} \langle v^2 \rangle \frac{d\langle U \rangle}{dy} \times (\langle u^2 \rangle^* - \langle u^2 \rangle) = 0 \tag{23}$$

Since $\langle u^2 \rangle^* \neq \langle u^2 \rangle$ generally, $\langle uv \rangle^*$ cannot remain the same as the prescribed value. The only way to resolve this is to set $\gamma_5 = 0$.

Another combination is $\langle u^2 \rangle^* = \langle u^2 \rangle, \langle v^2 \rangle^* = \langle v^2 \rangle$, then

$$-\frac{1}{k} C_1 \epsilon \langle u^2 \rangle + 2 C_2 \frac{d\langle U \rangle}{dy} \langle uv \rangle^* + C_0 \epsilon - \gamma_5 \frac{\langle u^2 \rangle}{k} \frac{d\langle U \rangle}{dy} (\langle uv \rangle - \langle uv \rangle^*) = 0 \tag{24}$$

$$-\frac{1}{k} C_1 \epsilon \langle v^2 \rangle + C_0 \epsilon - \gamma_5 \frac{\langle v^2 \rangle}{k} \frac{d\langle U \rangle}{dy} (\langle uv \rangle^* - \langle uv \rangle) = 0 \tag{25}$$

$$-\frac{1}{k} C_1 \epsilon \langle uv \rangle^* + C_2 \frac{d\langle U \rangle}{dy} \langle v^2 \rangle = 0 \tag{26}$$

Unlike the first choice, the consistency cannot be satisfied even with the enforcement of $\gamma_5 = 0$. Therefore, we consider the first case only in our study. From this, we obtain a dispersion model in very simple form.

$$du = \left(-\frac{1}{2k} C_1 \epsilon u + C_2 \frac{d\langle U \rangle}{dy} v \right) dt + \sqrt{C_0 \epsilon}\, dW_1 \tag{27}$$

$$dv = -\frac{1}{2k} C_1 \epsilon v\, dt + \sqrt{C_0 \epsilon}\, dW_2 \tag{28}$$

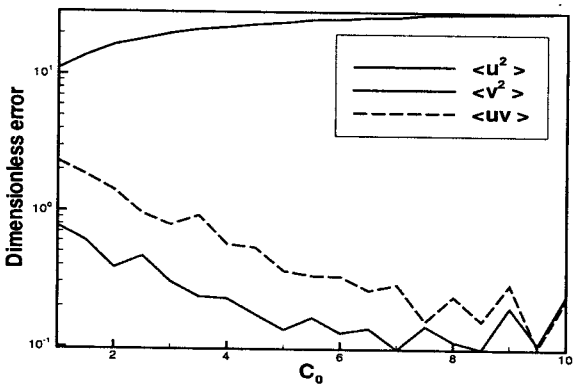

Figure 1: Dimensionless error defined by $\int [\langle u_i u_j \rangle - \langle u_i u_j \rangle_{exact}]^2 \, dy / \int \langle u_i u_j \rangle^2_{exact} \, dy$

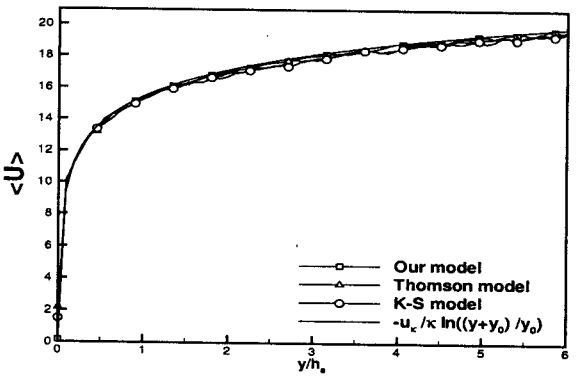

Figure 2: A comparison of mean velocity of three models with log mean velocity profile $\frac{u_\tau}{\kappa} \ln \frac{(y+y_0)}{y_0}$

with the relation between C_0, C_1 and C_2 as listed in the last row of Table 1. Note that constants C_1,C_2 are functions of C_0 which is only one remaining model parameter. To numerically ensure that the desired Reynolds stresses be maintained to be the given values, the error of the computed stresses is shown in terms of C_0 in Fig. 1. As expected, the error for the wall-normal and shear components remain small, whereas the streamwise component shows large error. In the investigated range of C_0, the behavior of the error suggests the existence of an optimum value of C_0. From the performance of the model in dispersion prediction, the optimum value turned out to be 4, for which the errors for all three Reynolds stresses including the streamwise component remain reasonably small.

DISPERSION RESULTS

In this section we present results for dispersion of our model and other known models with experimental data of Raupach and Legg (1983). In the experiment, the line source heating was used to simulate concentrated source. Equations (2,27,28) are numerically integrated by using the 3rd-order Runge-Kutta scheme, with a varying time step $\Delta t = \alpha \tau_L$, where $\tau_L = 2\sqrt{\langle v \rangle^2}/C_0\epsilon$ is the Lagrangian time scale. For the numerical stability and to avoid singularity at the wall, $\alpha = 0.02$ was sufficient (Kurbanmuradov and Sabelfeld, 2000). The elastic reflection boundary condition is used when a particle hits the wall. In this paper, for the best model performance we set C_0 to 4 for our model. Compared models are the models by Kurbanmuradov and Sabelfeld

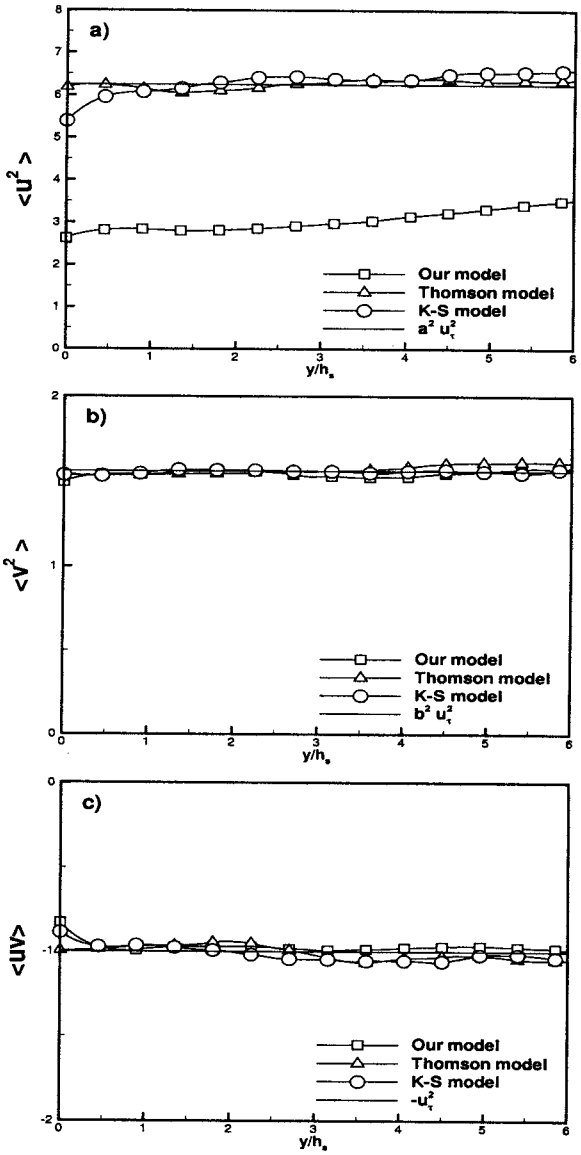

Figure 3: A comparison of Reynolds stress of our model with other model at $x/h_s = 30$.

(2000) (K-S model) and by Thomson (1987). We set $C_0 = 4$ for K-S model, $C_0 = 5$ for the Thomson model. In Fig. 2 the computed ensemble-averaged velocity profiles at downstream location $x/h_s = 30$ are plotted against dimensionless wall distance y/h_s, where h_s is the height of the source. All models follow the exact mean flow very well with a slight underprediction. We examine the normal stresses and shear stress at the same downstream location in Fig. 3. Thomson's model and K-S model produce $\langle u^2 \rangle$, $\langle v^2 \rangle$ and $\langle uv \rangle$ qualitatively well. Our model shows a large discrepancy in the $\langle u^2 \rangle$ which is expected. However, $\langle v^2 \rangle$ and $\langle uv \rangle$ show good agreement with the exact value.

In Fig. 4, the normalized mean concentration, $\bar{c}/c^*$ at several downstream locations, $x/h_s = 2.5$, 7.5, 15, 30 are illustrated. Here, $\bar{c}$ is the mean concentration and $c^* = Q/(h_s \langle U(h_s) \rangle)$ where Q is the line source strength per unit length. Right after the particles are released, the prediction by all models is excellent in terms of the peak value and position. At $x/h_s = 7.5$, however, all models slightly overestimate the concentration and the peak of concentration is slightly different from the measurement. Our model

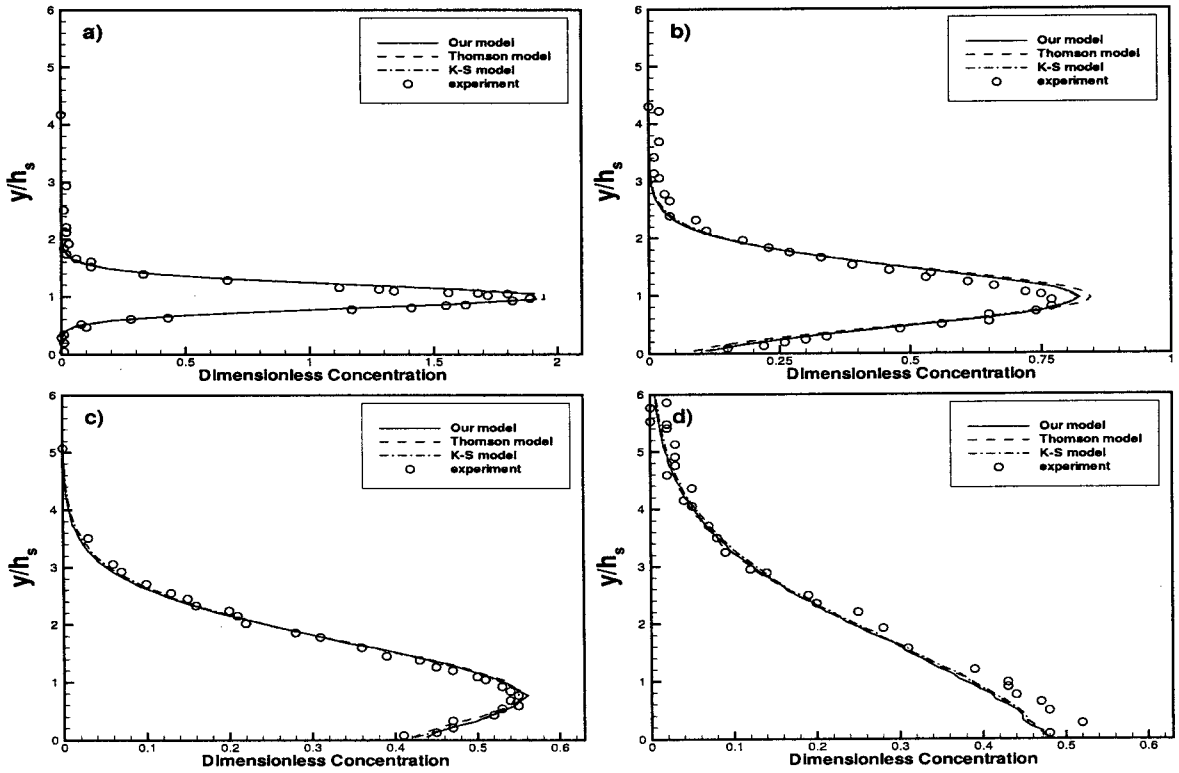

Figure 4: Dimensionless concentration $\overline{c}/c^*$ at four locations: (a) x/h_s= 2.5; (b) x/h_s= 7.5; (c) x/h_s= 15; (d) x/h_s= 30 compared with experimental data (Raupach and Legg, 1983)

and K-S model outperform the Thomson's model in terms of the peak value and near-wall concentration, but differences are minor. At $x/h_s = 15$, all tested models exhibit excellent performances. At $x/h_s = 30$, however, all models underestimate the concentration near the wall. Overall, the performance of the tested models for concentration is excellent.

In Fig. 5, the normalized horizontal flux ($=\overline{uc'}/u_\tau c^*$) for each model is illustrated with the experimental data. Despite a poor estimation of $\langle u^2 \rangle$, our model's prediction for the horizontal flux is relatively good compared to other models. Thomson's model and K-S model have shown a very similar behavior in the prediction of the Reynolds normal stresses but their horizontal flux are significantly different. Unexpectedly, our model's result is very close to Thomson's model. The vertical fluxes are plotted in Fig. 6. Although all models show good agreement with the measurement at all position, our model slightly outperforms other models, specially at $x/h_s = 15$.

CONCLUSION

A new Lagrangian dispersion model based on the Generalized Langevin Model corresponding to the Isotropization of Production Model is constructed under physically plausible assumptions. We use the elliptic-relaxation to incorporate anisotropic effect into the GLM. Using the self-similarity and analytical solution of the elliptic-relaxation, the model parameters of the present dispersion model are expressed in terms of C_0. However, the streamwise Reynolds stress of the computed velocity is not maintained to be the same as the prescribed value due to the inconsistency nature of our model. Despite this inconsistency, our model shows good agreement with the experiment results in the prediction of concentration and fluxes.

REFERENCES

Dreeben, T. D., and Pope, S. B., 1998, "Probability density function/Monte Carlo Simulation of Near-wall Turbulent Flows," *J. Fluid Mech.*, Vol. 357, pp. 141-166.

Dreeben, T. D., and Pope, S. B., 1997, "Pdf and Reynolds-stress Modeling of Near-wall Turbulent Flows," *Phys. Fluids*, Vol. 9, pp. 154-163.

Durbin, P. A., 1991, "Near-Wall Turbulence Closure Modeling Without "Damping Function"," *Theoret. Comput. Fluid Dynamics.*, Vol. 3, pp. 1-13.

Haworth, D. C., and Pope, S. B., 1986, "A Generalized Langevin Model for Turbulent Flows," *Phys. Fluids*, Vol. 29, pp. 387-405.

Kurbanmuradov, O., and Sabelfeld, K., 2000, "Lagrangian Stochastic Models for Turbulent Dispersion in The Atmospheric Boundary Layer," *Boundary-Layer Meteorology*, Vol. 97, pp. 191-218.

Pope, S. B., 1994, "On the Relationship between Stochastic Lagrangian Models of Turbulence and Second-moment Closures," *Phys. Fluids*, Vol. 6, pp. 973-985

Raupach, M. R., and Legg, B. J., 1983, "Turbulent Dispersion from an Elevated Line Source," *J. Fluid Mech.*, Vol. 136, pp. 111-137.

Reynolds, A. M. 1998a, "On the Formulation of Lagrangian Stochastic Models of Scalar Dispersion within Plant Canopies," *Boundary-Layer Meteorology*, Vol. 86, pp. 333-344.

Reynolds, A. M. 1998b, "On Trajectory Curvature as a Selection Criterion for Valid Lagrangian Stochastic Dispersion Models," *Boundary-Layer Meteorology*, Vol. 88, pp. 77-86.

Thomson, D. J., 1987, "Criteria for the selection of stochastic models of particle trajectories in turbulent flows," *J. Fluid Mech*, Vol. 180, pp. 529-556.

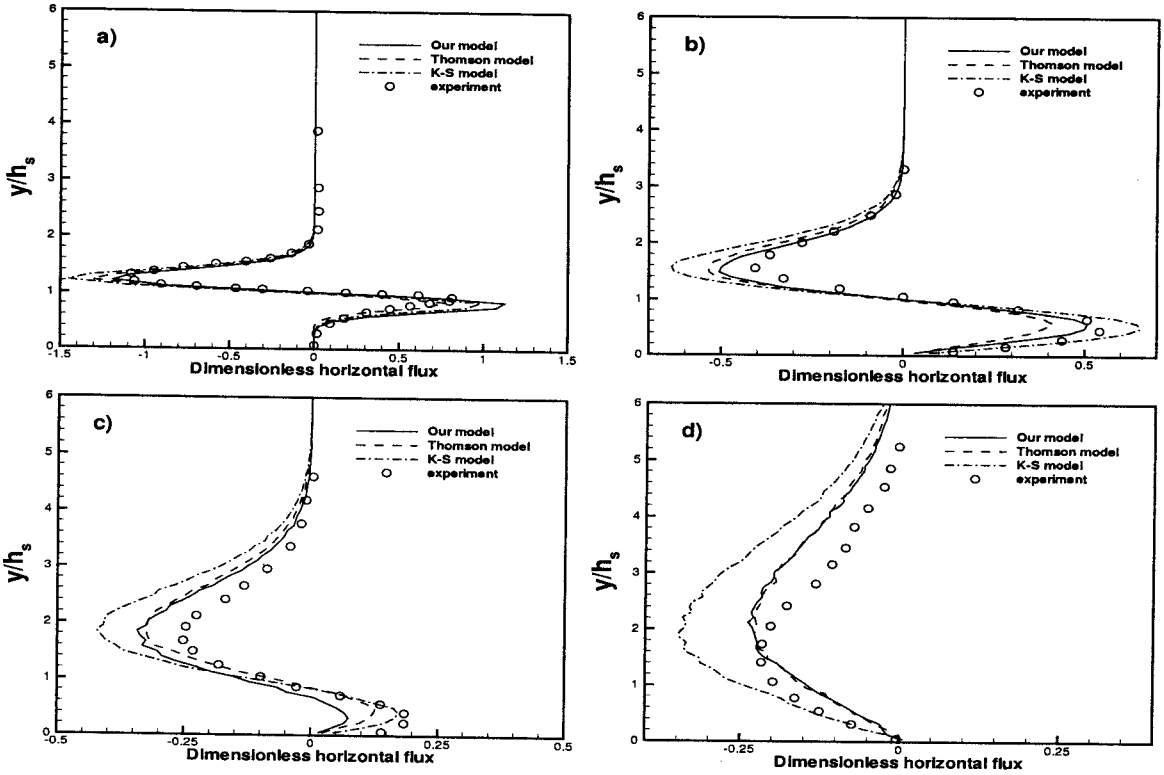

Figure 5: Dimensionless horizontal flux $\overline{uc'}/u_\tau c^*$ at locations: (a) x/h_s= 2.5; (b) x/h_s= 7.5; (c) x/h_s= 15; (d) x/h_s= 30 compared with experimental data (Raupach and Legg, 1983)

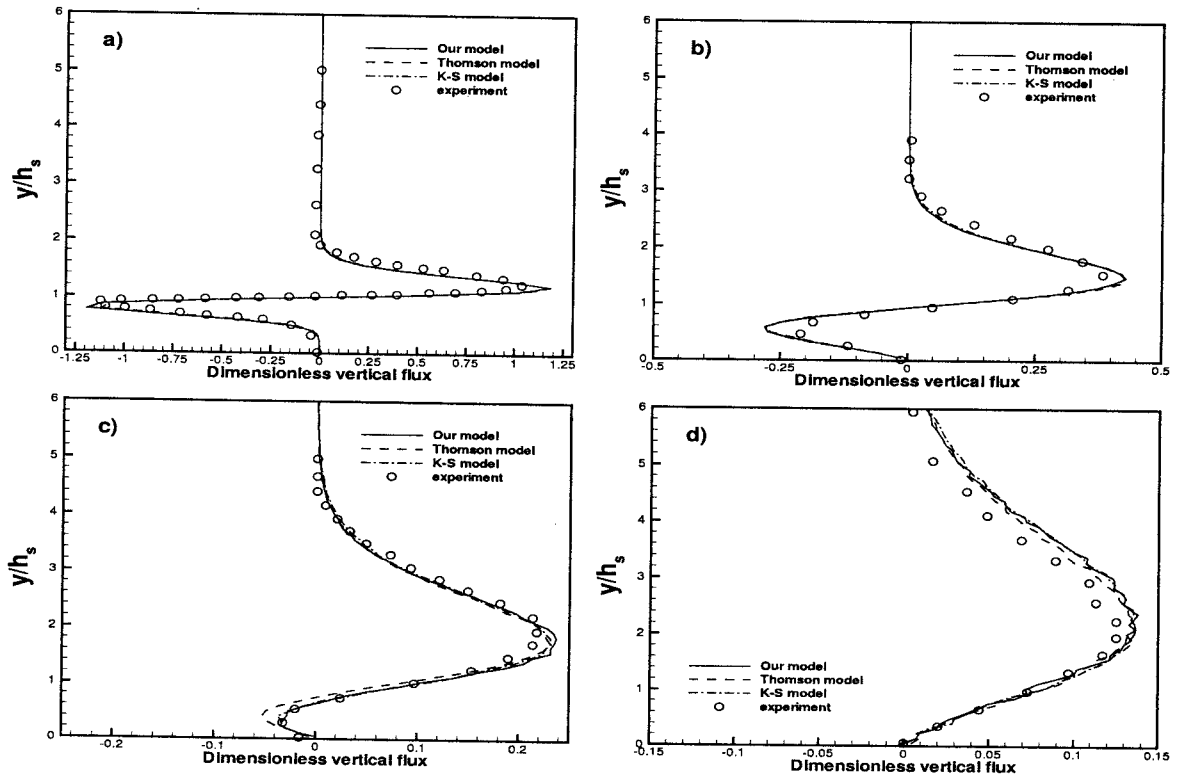

Figure 6: Dimensionless vertical flux $\overline{vc'}/u_\tau c^*$ at locations: (a) x/h_s= 2.5; (b) x/h_s= 7.5; (c) x/h_s= 15; (d) x/h_s= 30 compared with experimental data (Raupach and Legg, 1983)